Signatures of a Spin-$\frac{1}{2}$ Cooperative Paramagnet in the Diluted Triangular Lattice of Y_2CuTiO_6

S. Kundu,[1,‡] Akmal Hossain,[2,‡] Pranava Keerthi S.,[2] Ranjan Das,[2] M. Baenitz,[3] Peter J. Baker,[4] Jean-Christophe Orain,[5] D. C. Joshi,[6] Roland Mathieu,[6] Priya Mahadevan,[7] Sumiran Pujari,[1] Subhro Bhattacharjee,[8] A. V. Mahajan,[1,*] and D. D. Sarma[2,†]

[1]*Department of Physics, Indian Institute of Technology, Bombay, Powai, Mumbai 400076, India*
[2]*Solid State and Structural Chemistry Unit, Indian Institute of Science, Bengaluru 560012, India*
[3]*Max Planck Institute for Chemical Physics of Solids, 01187 Dresden, Germany*
[4]*ISIS Pulsed Neutron and Muon Source, STFC Rutherford Appleton Laboratory, Harwell Campus, Didcot, Oxfordshire OX110QX, United Kingdom*
[5]*Paul Scherrer Institute, Bulk MUSR group, LMU 5232 Villigen PSI, Switzerland*
[6]*Department of Engineering Sciences, Uppsala University, Box 534, SE-751 21 Uppsala, Sweden*
[7]*S. N. Bose National Center for Basic Sciences, Block-JD, Salt Lake, Kolkata-700106, India*
[8]*International Centre for Theoretical Sciences, Tata Institute of Fundamental Research, Bengaluru 560089, India*

(Received 19 March 2020; revised 11 June 2020; accepted 4 August 2020; published 9 September 2020)

We present a combination of thermodynamic and dynamic experimental signatures of a disorder driven dynamic cooperative paramagnet in a 50% site diluted triangular lattice spin-$\frac{1}{2}$ system: Y_2CuTiO_6. Magnetic ordering and spin freezing are absent down to 50 mK, far below the Curie-Weiss scale ($-\theta_{CW}$) of $\sim$134 K. We observe scaling collapses of the magnetic field and temperature dependent magnetic heat capacity and magnetization data, respectively, in conformity with expectations from the random singlet physics. Our experiments establish the suppression of any freezing scale, if at all present, by more than 3 orders of magnitude, opening a plethora of interesting possibilities such as *disorder stabilized* long range quantum entangled ground states.

DOI: 10.1103/PhysRevLett.125.117206

Conventional wisdom suggests that structural disorder in magnetic insulators usually leads to random spin-spin exchanges, which, in turn, promote spin freezing at low temperatures [1–3]. There is, however, an interesting alternative where quenched randomness may promote competing magnetic interactions and quantum fluctuations, thereby enhancing the possibility of realizing quantum spin liquids (QSLs) [4], as recently suggested for $Ba_3CuSb_2O_9$ [5] and $Pr_2Zr_2O_7$ [6].

This raises several interesting and experimentally relevant questions: Can structural disorder in magnetic insulators enhance quantum fluctuations and drive a magnetically ordered state (in clean limit) to a quantum paramagnet? What then is the nature of such a paramagnet? Can such a state support nontrivial many-body entanglement and realize a disorder driven QSL [7,8]? This possibility of realizing QSLs [9–11] and associated novel superconductors [12] arising from the interplay of disorder and interactions near the metal-insulator transition was explored theoretically in the context of doped semiconductors and boron doped diamond. On the experimental front, low temperature dynamic paramagnetism was observed in the irradiation induced disordered organic magnet κ-$(ET)_2Cu[N(CN)_2]Cl$ [8]. However, the question of a disorder driven QSL is different from that of the effect of disorder in a clean QSL. In the latter case, the QSL is often stable to at least dilute local impurities, albeit with interesting defect states [13–18].

These issues are particularly pertinent for two-dimensional spin-$\frac{1}{2}$ frustrated magnets where reduced dimensionality enhances quantum fluctuations and suppresses ordering tendencies. Thus, these systems serve as natural platforms to realize QSLs as in candidate materials Herbertsmithite ($ZnCu_3(OH)_6Cl_2$) [19–24] and κ-$(ET)_2Cu_2(CN)_3$ [25]. Notably, in Herbertsmithite, QSL is suggested to be stable to off-plane Cu^{2+} magnetic disorder [26,27]. Similarly, in three-dimensional hyperkagome QSL candidate $Na_4Ir_3O_8$ [28,29], the coexistence of slow timescales and signatures of quantum fluctuations has been observed [30].

In this Letter, we report an experimental realization of a dynamic cooperative paramagnet in a spin-$\frac{1}{2}$ magnet on a site diluted triangular lattice Y_2CuTiO_6 (YCTO) [31,32]. This is established by the absence of any ordered or frozen magnetism down to the lowest accessible temperature (50 mK) despite substantial magnetic interactions indicated by a large Curie-Weiss temperature ($\theta_{CW} \sim -134$ K) and disorder in the system. YCTO, therefore, is an example of a disordered triangular lattice magnet with 50:50 random mixture of spin-$\frac{1}{2}$ Cu^{2+} atoms and nonmagnetic Ti^{4+} atoms,

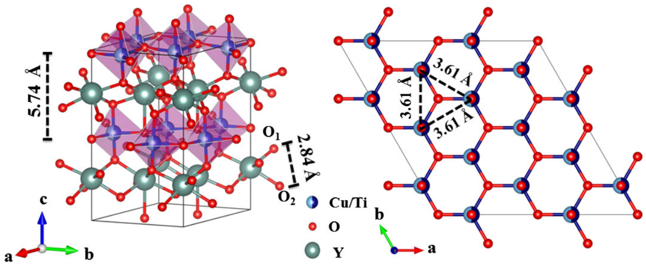

FIG. 1. Double perovskite structure with one unit cell of Y_2CuTiO_6 and corner-shared polyhedra of $(Cu/Ti)O_5$ connected via oxygen atoms in the *ab* plane. The Cu^{2+}/Ti^{4+} ions form edge-shared triangles.

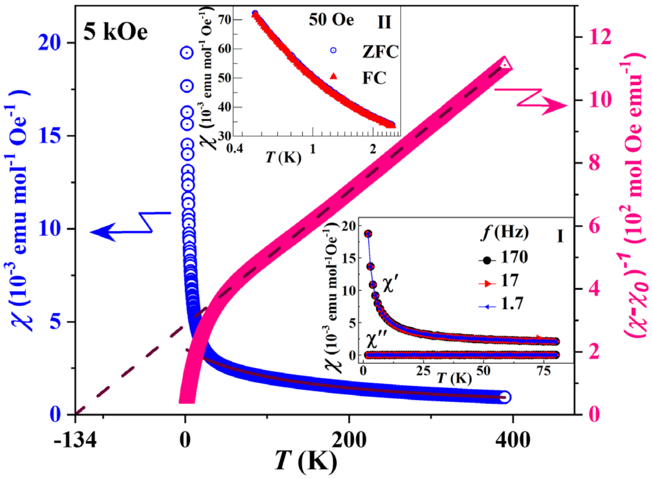

FIG. 2. The left *y* axis shows $\chi(T)$ (open blue circles) of Y_2CuTiO_6 and the right *y* axis shows the inverse susceptibility (open pink triangles) free from χ_0. The Curie-Weiss fit is shown in the *T* range 200–400 K with a solid line. The intercept on the *x* axis gives a θ_{CW} of about −134 K. Inset "I" shows the ac susceptibility for different frequencies till 2 K. Inset "II" shows the absence of any bifurcation in the ZFC/FC data in 50 Oe down to 500 mK.

as shown in the left frame of Fig. 1. We observe a specific scaling behavior of thermodynamic quantities [1,33–36] indicating a low temperature dynamic spin-$\frac{1}{2}$ paramagnet with possible formation of random singlets that survive down to the lowest accessible temperature [37].

In YCTO, each Cu/Ti site is surrounded by a triangular bipyramid of five oxygen atoms with three in the basal (*ab*) plane and two along the *c* axis. The resultant $(Cu/Ti)O_5$ units arranged in a triangular lattice in the (*ab*) plane are well-separated by an intervening layer of nonmagnetic Y^{3+} ions along the *c* axis with a large interlayer separation of ~5.7 Å. The exchange interaction strengths between nearest neighbor Cu atoms in the (*ab*) plane (J_{nn}) and the interlayer magnetic coupling (J_c) were calculated using density functional theory [see Supplemental Material (SM) [40] for calculation details]. J_{nn}/k_B and J_c/k_B were determined to be ~ -33.6 K and ~ -1.0 K, respectively. These estimates lead to a calculated $\theta_{\rm CW}$ of ~ -104 K in reasonable agreement with the experimental value of −134 K. Larger than an order of magnitude anisotropy in magnetic interactions indicates that two-dimensional triangular lattices of corner-shared $(Cu/Ti)O_5$ units, as shown in the right frame of Fig. 1, are coupled only weakly along the *c* axis. Thus, we may think of the system approximately as one spin-$\frac{1}{2}$ at each Cu^{2+} site sitting on an isotropic triangular lattice that is 50% diluted with nonmagnetic Ti^{4+} ions. Experimentally, no superlattice formation is observed in spite of the charge difference of the Cu^{2+} and Ti^{4+} ions with the structural uniformity achieved only at a statistical level. We also note that superlattice formations on a triangular motif are geometrically frustrated at 50% dilution [58]. Thus, YCTO, to a very good approximation, is a randomly 50% diluted spin-rotation invariant spin-$\frac{1}{2}$ magnet on a triangular lattice. Note that the random in-plane dilution and the spin-rotation symmetry are the two key differences between YCTO and the recently much investigated $YbMgGaO_4$ [7,59].

Polycrystalline samples of YCTO were synthesized by standard solid state reaction techniques. Details of the sample preparation and measurements [magnetization, heat capacity, ^{89}Y nuclear magnetic resonance (NMR), and muon spin relaxation (μSR)] are presented in the Supplemental Material [40]. From Rietveld refinements of x-ray diffraction data (see the SM [40] for details), we confirmed that YCTO crystallizes in the noncentrosymmetric hexagonal structure with the space group $P6_3cm$ [31,32] isostructural to $LuMnO_3$ [60].

The dc susceptibility $\chi(T) = M(T)/H$ as a function of *T* is shown in Fig. 2, where no signature of any magnetic ordering is seen down to 2 K. The divergence of χ at lowest temperatures is well-known to generally arise from the presence of a minor fraction (~2% in the present case) of free spins in many such systems, as detailed in the SM [40]. A fitting of the high temperature (200–400 K) dc susceptibility to a Curie-Weiss form $\chi = \chi_0 + C/(T - \theta_{\rm CW})$—where χ_0, *C*, and $\theta_{\rm CW}$ are the temperature independent Van Vleck paramagnetic and core diamagnetic susceptibilities, the Curie constant, and the Curie-Weiss temperature, respectively—yields $\chi_0 = 3.48 \times 10^{-4}$ emu mol^{-1} Oe^{-1}, $C = 0.47$ emu K mol^{-1} Oe^{-1}, and $\theta_{\rm CW} = -134$ K. The value of $\theta_{\rm CW}$ is in agreement with earlier reports [31,61], and the inferred moment of $\mu_{\rm eff} = 1.94\ \mu_B$ is consistent with the expected value of ~1.9 μ_B for a spin $S = \frac{1}{2}$ Cu^{2+} system with $g = 2.2$, as reported for many cuprates. The large and negative $\theta_{\rm CW}$ suggests substantial antiferromagnetic spin-spin interactions within each triangular layer.

The real and the imaginary parts of the ac susceptibility (see inset "I" of Fig. 2) did not show any indication of magnetic ordering. Further, the lack of frequency dependence of the ac susceptibility over a range of frequencies

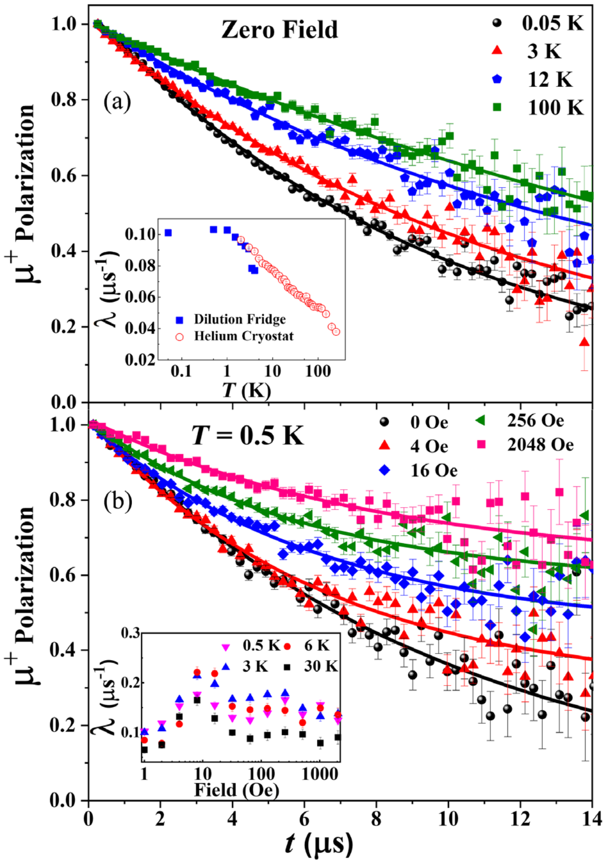

FIG. 3. (a) Muon depolarization with time shown for various temperatures at zero fields. Solid lines are fits as described in the text. The inset shows the variation of the obtained muon relaxation rate with temperature. (b) Muon depolarization for various longitudinal fields at 0.5 K. The corresponding inset shows the variation of the obtained muon relaxation rate with field.

indicates the absence of spin-freezing down to 2 K. The lack of freezing despite extensive disorder is reemphasized by the absence of any irreversibility between the Field Cooled (FC) and Zero Field Cooled (ZFC) magnetization data at a low field (50 Oe) (see inset "II" of Fig. 2), also ruling out any magnetic ordering down to 500 mK. Thus, this system with substantial antiferromagnetic interactions on an essentially two-dimensional triangular lattice with spin-$\frac{1}{2}$s and a relatively small spin-orbit coupling strength with no evidence of any magnetic ordering or freezing down to 500 mK offers a unique opportunity to probe a dynamic low temperature correlated paramagnetic phase that can possibly harbor an intricate interplay of quantum fluctuations and disorder.

We extend the limit of the low temperature probe down to 50 mK with μSR experiments. Figure 3(a) shows smooth exponential depolarization of muon spins without any oscillations at all temperatures in the absence of an external magnetic field. This shows that the fluctuation frequency of the local fields is much greater than the μSR frequency, ruling out any static magnetic ordering down to 50 mK, though it cannot rule out a dynamic magnetic order [62]. We fit the muon spin polarization data to $e^{-\lambda t}$, as detailed in the SM [40], and obtain the muon spin relaxation rate λ, plotted as a function of the temperature in the inset of Fig. 3(a). We note that for a random internal static magnetic field with Gaussian distribution and zero mean, one expects a muon signal to decay as e^{-at^2} (a = constant), which is different from the $e^{-\lambda t}$ dependence seen in our experiments [63].

The initial increase in λ [see inset of Fig. 3(a)] on cooling indicates the expected slowing down of spin dynamics of Cu moments with a lowering of temperature down to about 2 K, below which it essentially levels off at a value of $\lambda \approx 0.1\ \mu s^{-1}$ down to ~50 mK. This indicates a dynamic low temperature state [64,65]. If the observed muon depolarization arises from any static internal magnetic fields, $\lambda \approx 0.1\ \mu s^{-1}$ would suggest an estimate of that field ($\simeq 2\pi\lambda/\gamma_\mu$, with γ_μ being the muon gyromagnetic ratio) to be about 7.4 Oe. Then the muon spins can be decoupled from the static moments with the application of a longitudinal field of a magnitude which is about ten times this internal field [63]. We have measured the muon polarization as a function of time at various temperatures and applied longitudinal fields up to 2048 Oe—about 270 times larger than 7.4 Oe—yet we did not observe the total suppression of muon depolarization. This indicates the existence of strongly fluctuating local magnetic fields in the system. A set of representative data obtained at 500 mK is shown in Fig. 3(b). The corresponding decay constants λ are shown in the inset to Fig. 3(b) as a function of the applied field for different temperatures. At all measured temperatures, λ is nearly constant apart from a peak around 10 Oe, which is presumably due to a quadrupolar level crossing resonance [66] coming from the neighboring copper nuclei. This temperature independence suggests rapid spin fluctuations and the absence of any spin ordering or freezing down to at least 50 mK despite sizable magnetic interactions.

This observation of the absence of spin freezing or magnetic ordering down to 50 mK then raises the interesting possibility of realizing disorder driven quantum paramagnetism in YCTO. The lack of spin ordering or freezing down to a very low temperature is also emphasized in the total heat capacity $C_p(T)$ (see the SM [40]), measured down to 350 mK for various magnetic fields. The total contribution C_s of all spins to the specific heat is estimated by subtracting the lattice contribution, C_{lat}, from C_p. We find $C_s/T \approx 0$ by 20 K [see inset to Fig. 4(a)]. Spin entropy estimated by integrating C_s/T vs T up to 20 K is shown in Fig. 4(a) for different applied magnetic fields. Clearly, this procedure accounts for only about 15% of the total spin entropy per mole of spin-$\frac{1}{2}$ Cu ions, evidencing a huge unquenched spin entropic content down to the lowest temperatures (350 mK) and complementing the muon

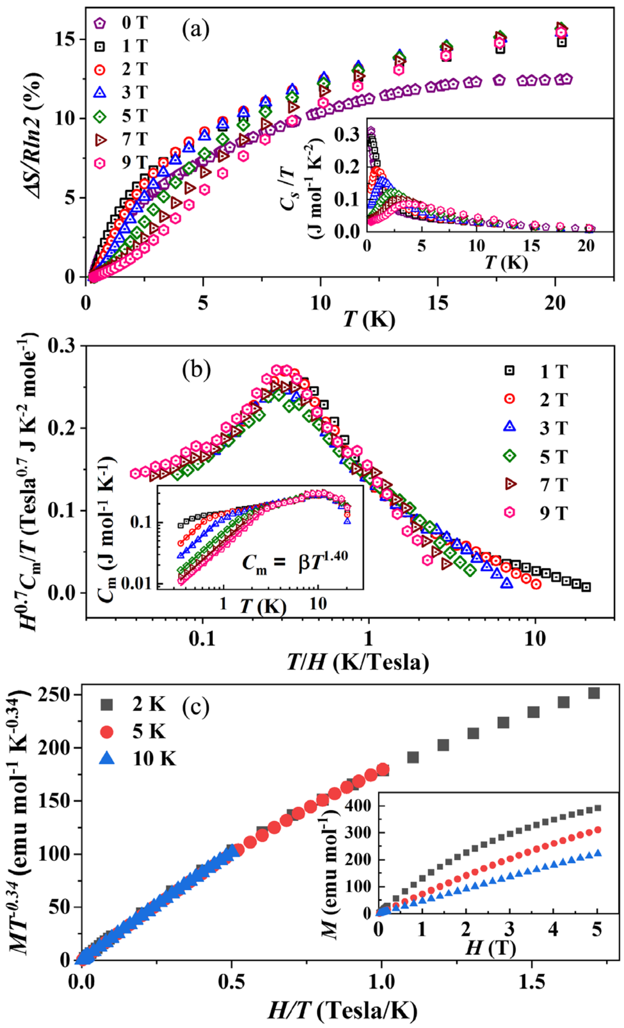

FIG. 4. (a) The change in the spin entropy ΔS as a function of temperature between 350 mK and 20 K. In the presence of a magnetic field, marginally more entropy is released, indicating a possible partial lifting of frustration by the Zeeman field, another canonical signature of cooperative magnets such as spin ice [67]. The inset shows the spin contributions to the specific heat $(C_s = C_p - C_{\mathrm{lat}})/T$ vs T over the same range. (b) The scaled magnetic heat capacity $H^\gamma C_m/T$ of YCTO is plotted against the scaled temperature T/H for various applied fields H. The data collapse in the low temperature regime is consistent with the q $= 0$ form of the universal function of Ref. [27], which is expected in absence of spin-orbit coupling. The inset shows the C_m of YCTO after deduction of the lattice and Schottky contributions. (c) The M(H) isotherm has been scaled in the form of $MT^{-\alpha}$ vs H/T.

relaxation data. We can further remove the contribution of free spins from C_s by subtracting the Schottky terms as detailed in the SM [40], thereby defining C_m. The inset to Fig. 4(b) shows the T dependence of C_m vs T at different fields on a log-log scale for better clarity in the low temperature region. The data clearly show that above ~2 K, C_m is independent of the applied magnetic field. Below 2 K, C_m follows a power law ($C_m \approx \beta T^{1.4}$), with temperature indicating the presence of a large number of low energy excitations. The regime of power-law behavior of C_m shrinks with a decreasing magnetic field to a fraction of a Kelvin for a field of 1 T, suggesting that the low energy excitations directly couple to the magnetic field, which is characteristic of random singlets with a distribution of bond energies [7,27].

With the above results, we now turn to investigate the nature of the low temperature, dynamic, correlated paramagnet. The primary in-plane superexchange between two nearest neighbor Cu^{2+} atoms is mediated by the intermediate in-plane oxygen, as is evident in Fig. 1. Further neighbor exchanges either involve more intermediate O^{2-} and in-plane Cu^{2+}/Ti^{4+} or out-of-plane Y^{3+} and hence are expected to be suppressed similar to the interplane magnetic exchanges. This indicates that the magnetic physics of YCTO can be understood within a minimal model of a diluted short-range antiferromagnet on a triangular lattice with a Hamiltonian: $H = \sum J_{\mathbf{rr}'}\eta_{\mathbf{r}}\eta_{\mathbf{r}'}\mathbf{S}_{\mathbf{r}} \cdot \mathbf{S}_{\mathbf{r}'}$, where $\mathbf{S}_{\mathbf{r}}$ are spin-$\frac{1}{2}$ operators on the triangular lattice sites $\mathbf{r}$ and $\eta_{\mathbf{r}} = 0(1)$ for a $Ti^{4+}(Cu^{2+})$ site [68,69]. The distribution of Ti^{4+} and Cu^{2+} in the 1:1 ratio is given by a probability distribution function $\mathcal{P}[\{\eta_{\mathbf{r}}\}]$. $J_{\mathbf{rr}'}$ denotes short range antiferromagnetic interactions between the Cu^{2+} ions, and the randomness of the position of Cu^{2+} leads to a distribution in $J_{\mathbf{rr}'}$ given by $\bar{\mathcal{P}}[\{J_{\mathbf{rr}'}\}]$, which is correlated with (but not necessarily same as) $\mathcal{P}[\{\eta_{\mathbf{r}}\}]$. The absence of signatures of formation of a superlattice or any other structural anomalies in diffraction experiments suggests $\mathcal{P}[\{\eta_{\mathbf{r}}\}]$ to have weak correlations among different sites. Therefore, we expect that $\bar{\mathcal{P}}[\{J_{\mathbf{rr}'}\}]$ has a relatively small width.

Due to the site dilution, YCTO is more similar to doped semiconductors [1,9,10] than the recently discovered $YbMgGaO_4$ [59]. However, in contrast to the low density of magnetic moments in doped semiconductors, YCTO has a dense (50%) concentration of spins. In the absence of any magnetic order, as established experimentally, the natural option for the system in such circumstances is to locally minimize energy of the antiferromagnetic exchanges by forming singlets. In the process of the formation of these singlets, a smaller number of spins are left over due to a lack of partners. However these spins, sitting on a random network, are not isolated because of the high density of the magnetic ions with which they interact. Indeed, if the background network of the dimers is dynamic, the positions of such unpaired spins are not even static [26]. These unpaired dynamic *quasispins* [70] then interact with each other with effective exchange interactions of the form $\mathcal{H}_{\mathrm{eff}} = \sum_{ij} \mathcal{J}_{ij}\mathbf{S}_i \cdot \mathbf{S}_j$, where the effective couplings are expected to be $|\mathcal{J}_{ij}| \sim e^{-|\mathbf{r}_i - \mathbf{r}_j|/\xi}$ where ξ is the underlying spin correlation length [7,70]. Thus, $\mathcal{J}_{ij}$ are weak and random, and the fate of the system crucially depends on their distribution as well as the sign structure. Owing to the lack of bipartite structure of the underlying triangular motif, these exchanges are expected to be a mixture of ferromagnetic and antiferromagnetic interactions, eventually leading to a spin-glass state at a much lower temperature [1,7,71] depending on the magnitude and distribution of $\mathcal{J}_{ij}$. A power-law distribution $\sim\mathcal{J}^{-\gamma}$ in these effective couplings leads to a magnetic specific heat scaling at a finite magnetic field of $C_m \sim TH^{-\gamma}$ for $T/H < 1$.

The heat capacity measurements reveal a power-law behavior with the universal scaling of the $H^{\gamma}C_m/T$ with T/H and $\gamma \simeq 0.7$ [Fig. 4(b)]. Indeed, recently such a scaling has been argued to result from an intermediate temperature random singlet phase in a bond disordered system [27,72]. The above conclusions are consistent with the finite dynamic rate observed in muon spin-relaxation experiments where the rate is fairly insensitive to the applied small external magnetic fields.

Further evidence of the correlated nature of the low temperature paramagnet comes from the magnetic field dependence of the magnetization at low temperatures [see inset of Fig. 4(c)], which cannot be described by a free spin Brillouin function. Analysis of the specific heat allows us to estimate the free spin magnetization. Having removed this contribution, the magnetization shows a scaling collapse of the form $MT^{-\alpha}$ (with $\alpha = 0.34 \pm 0.02$) as a function of H/T [see Fig. 4(c)] as expected for the above-mentioned power-law distribution of the effective exchanges with $\alpha = 1 - \gamma$ [26,27].

In summary, through a complementary set of experiments on the randomly 50% depleted triangular lattice $S = 1/2$ magnet Y_2CuTiO_6, we establish the absence of magnetic order and/or spin freezing down to 50 mK. This is 0.037% of the Curie-Weiss scale of about −134 K, the latter implying strong antiferromagnetic couplings between the magnetic Cu^{2+} spins. While spin freezing may occur at even lower temperatures, such drastic suppression of freezing compared to the Curie-Weiss scale opens up a cooperative paramagnetic regime, at least between 50 mK and 2 K. In the cooperative paramagnet, a scaling collapse, consistent with the random singlet phenomenology [27], is observed in the magnetic field dependent on specific heat and magnetization. An exciting question, fueled by our experimental observation of dynamical signatures, pertains to the role of quantum coherence in the cooperative paramagnet and in particular whether it can support the nontrivial entanglement expected in a QSL. While our existing understanding of *clean* frustrated magnets indicates that cooperative paramagnets provide the right background to look for QSLs, the search for such quantum coherence in Y_2CuTiO_6 is clearly a very interesting future step in exploring *disorder driven* QSLs. The issue of doping away from the 50% dilution or with carrier doping forms similar sets of interesting open questions.

The authors thank Kedar Damle for useful discussion. The author groups from IIT Bombay and IISc acknowledge support of measurement facilities in their respective institutions. Experiments at the ISIS Neutron and Muon Source were supported by a beamtime allocation RB1900000 from the Science and Technology Facilities Council. A. H. thanks the Department of Science and Technology, Government of India for support. A. H. also acknowledges the Newton Fund for supporting the visit to ISIS, UK. This work is partly based on experiments performed at the Swiss Muon Source, Paul Scherrer Institute, Villigen, Switzerland. S. P. acknowledges the support of IRCC, IIT Bombay (17IRCCSG011), and SERB, DST, India (SRG/2019/001419). S. B. acknowledges funding supports through the Department of Atomic Energy, Government of India, under Project No. 12-R&D-TFR-5.10-1100 and the Max Planck Partner group on strongly correlated systems at ICTS and SERB-DST (India) through project Grant No. ECR/2017/000504. D. C. J. and R. M. thank the Stiftelsen Olle Engkvist Byggmästare and the Swedish Research Council (VR). A. V. M., D. D. S., S. P., and S. B. acknowledge the hospitality and support of ICTS and APCTP during the 2nd Asia Pacific Workshop on Quantum Magnetism (Code: ICTS/apfm2018/11). D. D. S. thanks the Science and Engineering Research Board, Department of Science and Technology, Government of India, and the Jamsetji Tata Trust for their support of this research.

[*]Corresponding author.
mahajan@phy.iitb.ac.in
[†]Corresponding author.
sarma@iisc.ac.in
[‡]These authors contributed equally to this work

[1] R. N. Bhatt and P. A. Lee, Phys. Rev. Lett. **48**, 344 (1982).
[2] K. Binder and A. P. Young, Rev. Mod. Phys. **58**, 801 (1986).
[3] P. Nordblad, Phys. Scr. **88**, 058301 (2013).
[4] L. Balents, Nature (London) **464**, 199 (2010).
[5] A. Smerald and F. Mila, Phys. Rev. Lett. **115**, 147202 (2015).
[6] L. Savary and L. Balents, Phys. Rev. Lett. **118**, 087203 (2017).
[7] I. Kimchi, A. Nahum, and T. Senthil, Phys. Rev. X **8**, 031028 (2018).
[8] T. Furukawa, K. Miyagawa, T. Itou, M. Ito, H. Taniguchi, M. Saito, S. Iguchi, T. Sasaki, and K. Kanoda, Phys. Rev. Lett. **115**, 077001 (2015).
[9] A. C. Potter, M. Barkeshli, J. McGreevy, and T. Senthil, Phys. Rev. Lett. **109**, 077205 (2012).
[10] K. Voelker and S. Chakravarty, Phys. Rev. B **64**, 235125 (2001).
[11] K.-S. Kim, Phys. Rev. B **73**, 235115 (2006).
[12] G. Baskaran, J. Supercond. Novel Magn. **21**, 45 (2008).
[13] A. J. Willans, J. T. Chalker, and R. Moessner, Phys. Rev. Lett. **104**, 237203 (2010).
[14] A. J. Willans, J. T. Chalker, and R. Moessner, Phys. Rev. B **84**, 115146 (2011).

[15] A. Kolezhuk, S. Sachdev, R. R. Biswas, and P. Chen, Phys. Rev. B **74**, 165114 (2006).

[16] F. Trousselet, G. Khaliullin, and P. Horsch, Phys. Rev. B **84**, 054409 (2011).

[17] O. Petrova, P. Mellado, and O. Tchernyshyov, Phys. Rev. B **90**, 134404 (2014).

[18] G. J. Sreejith, S. Bhattacharjee, and R. Moessner, Phys. Rev. B **93**, 064433 (2016).

[19] P. Mendels, F. Bert, M. A. de Vries, A. Olariu, A. Harrison, F. Duc, J. C. Trombe, J. S. Lord, A. Amato, and C. Baines, Phys. Rev. Lett. **98**, 077204 (2007).

[20] J. S. Helton, K. Matan, M. P. Shores, E. A. Nytko, B. M. Bartlett, Y. Yoshida, Y. Takano, A. Suslov, Y. Qiu, J.-H. Chung, D. G. Nocera, and Y. S. Lee, Phys. Rev. Lett. **98**, 107204 (2007).

[21] T. Imai, E. A. Nytko, B. M. Bartlett, M. P. Shores, and D. G. Nocera, Phys. Rev. Lett. **100**, 077203 (2008).

[22] A. Olariu, P. Mendels, F. Bert, F. Duc, J. C. Trombe, M. A. de Vries, and A. Harrison, Phys. Rev. Lett. **100**, 087202 (2008).

[23] M. A. de Vries, J. R. Stewart, P. P. Deen, J. O. Piatek, G. J. Nilsen, H. M. Rønnow, and A. Harrison, Phys. Rev. Lett. **103**, 237201 (2009).

[24] T.-H. Han, M. R. Norman, J.-J. Wen, J. A. Rodriguez-Rivera, J. S. Helton, C. Broholm, and Y. S. Lee, Phys. Rev. B **94**, 060409(R) (2016).

[25] Y. Shimizu, K. Miyagawa, K. Kanoda, M. Maesato, and G. Saito, Phys. Rev. Lett. **91**, 107001 (2003).

[26] R. Singh, Phys. Rev. Lett. **104**, 177203 (2010).

[27] I. Kimchi, J. P. Sheckelton, T. M. McQueen, and P. A. Lee, Nat. Commun. **9**, 4367 (2018).

[28] Y. Okamoto, M. Nohara, H. Aruga-Katori, and H. Takagi, Phys. Rev. Lett. **99**, 137207 (2007).

[29] Y. Singh, Y. Tokiwa, J. Dong, and P. Gegenwart, Phys. Rev. B **88**, 220413(R) (2013).

[30] R. Dally, T. Hogan, A. Amato, H. Luetkens, C. Baines, J. Rodriguez-Rivera, M. J. Graf, and S. D. Wilson, Phys. Rev. Lett. **113**, 247601 (2014).

[31] D. Choudhury, A. Hazarika, A. Venimadhav, C. Kakarla, K. T. Delaney, P. S. Devi, P. Mondal, R. Nirmala, J. Gopalakrishnan, N. A. Spaldin, U. V. Waghmare, and D. D. Sarma, Phys. Rev. B **82**, 134203 (2010).

[32] N. Floros, J. T. Rijssenbeek, A. B. Martinson, and K. R. Poeppelmeier, Solid State Sci. **4**, 1495 (2002).

[33] D. S. Fisher, Phys. Rev. B **50**, 3799 (1994).

[34] R. N. Bhatt and P. Lee, J. Appl. Phys. **52**, 1703 (1981).

[35] M. A. Paalanen, J. E. Graebner, R. N. Bhatt, and S. Sachdev, Phys. Rev. Lett. **61**, 597 (1988).

[36] C. Dasgupta and S.-k. Ma, Phys. Rev. B **22**, 1305 (1980).

[37] In the literature, there are at least two separate mentions of random singlet states in disordered quantum magnets. One is that of Ref. [7] with quenched disorder on which Ref. [27] is based. For strong disorder, the picture is that of pinned short range valence bonds in the background, with topological spin-$\frac{1}{2}$ defects that experience power-law distributed interactions [$p(J) \propto J^{-\gamma}$], as in Ref. [27], leading to the low energy phenomenology. The other scenario considered is the presence of strong exchange disorder in triangular lattices, as in Ref. [38,39].

[38] K. Watanabe, H. Kawamura, H. Nakano, and T. Sakai, J. Phys. Soc. Jpn. **83**, 034714 (2014).

[39] T. Shimokawa, K. Watanabe, and H. Kawamura, Phys. Rev. B **92**, 134407 (2015).

[40] See Supplemental Material, which includes Refs. [41–57], at http://link.aps.org/supplemental/10.1103/PhysRevLett.125.117206 for more details.

[41] D. D. Sarma *et al.* (2018) https://doi.org/10.5286/isis.e.95256627.

[42] P. E. Blöchl, Phys. Rev. B **50**, 17953 (1994).

[43] G. Kresse and D. Joubert, Phys. Rev. B **59**, 1758 (1999).

[44] G. Kresse and J. Furthmüller, Comput. Mater. Sci. **6**, 15 (1996).

[45] J. P. Perdew, K. Burke, and M. Ernzerhof, Phys. Rev. Lett. **77**, 3865 (1996).

[46] M. Imada, A. Fujimori, and Y. Tokura, Rev. Mod. Phys. **70**, 1039 (1998).

[47] A. Macridin, M. Jarrell, T. Maier, and G. A. Sawatzky, Phys. Rev. B **71**, 134527 (2005).

[48] Y. Mizuno, T. Tohyama, S. Maekawa, T. Osafune, N. Motoyama, H. Eisaki, and S. Uchida, Phys. Rev. B **57**, 5326 (1998).

[49] S. L. Dudarev, G. A. Botton, S. Y. Savrasov, C. J. Humphreys, and A. P. Sutton, Phys. Rev. B **57**, 1505 (1998).

[50] C. Zhong, X. Jiang, H. Yu, Q. Jiang, J. Fang, and Z. Li, J. Magn. Magn. Mater. **321**, 1260 (2009).

[51] I. V. Solovyev, M. V. Valentyuk, and V. V. Mazurenko, Phys. Rev. B **86**, 054407 (2012).

[52] J. A. Quilliam, F. Bert, A. Manseau, C. Darie, C. Guillot-Deudon, C. Payen, C. Baines, A. Amato, and P. Mendels, Phys. Rev. B **93**, 214432 (2016).

[53] A. Nag, S. Middey, S. Bhowal, S. K. Panda, R. Mathieu, J. C. Orain, F. Bert, P. Mendels, P. G. Freeman, M. Mansson *et al.*, Phys. Rev. Lett. **116**, 097205 (2016).

[54] R. Nath, K. Ranjith, B. Roy, D. Johnston, Y. Furukawa, and A. Tsirlin, Phys. Rev. B **90**, 024431 (2014).

[55] L. Clark, G. Sala, D. D. Maharaj, M. B. Stone, K. S. Knight, M. T. Telling, X. Wang, X. Xu, J. Kim, Y. Li *et al.*, Nat. Phys. **15**, 262 (2019).

[56] B. Gao, T. Chen, D. W. Tam, C.-L. Huang, K. Sasmal, D. T. Adroja, F. Ye, H. Cao, G. Sala, M. B. Stone *et al.*, Nat. Phys. **15**, 1052 (2019).

[57] Y. S. Choi, C. H. Lee, S. Lee, S. Yoon, W.-J. Lee, J. Park, A. Ali, Y. Singh, J.-C. Orain, G. Kim *et al.*, Phys. Rev. Lett. **122**, 167202 (2019).

[58] The lowest electrostatic energy configuration space of the Ti^{4+} and Cu^{2+} ions is highly degenerate. This is easiest to see by mapping to frustrated classical Ising configurations on the triangular lattice. We also note that the system is not at the percolation threshold despite 50% occupancy of the triangular lattice due to the presence of further neighbor magnetic exchange interactions, as discussed later in the text.

[59] Y. Li, H. Liao, Z. Zhang, S. Li, F. Jin, L. Ling, L. Zhang, Y. Zou, L. Pi, Z. Yang *et al.*, Sci. Rep. **5**, 16419 (2015).

[60] H. L. Yakel, W. C. Koehler, E. F. Bertaut, and E. F. Forrat, Acta Crystallogr. **16**, 957 (1963).

[61] K. Singh, N. Kumar, B. Singh, S. D. Kaushik, N. K. Gaur, S. Bhattacharya, S. Rayaprol, and C. Simon, J. Supercond. Novel Magn. **24**, 1829 (2011).

[62] P. Dalmas de Réotier, A. Yaouanc, L. Keller, A. Cervellino, B. Roessli, C. Baines, A. Forget, C. Vaju, P. C. M. Gubbens, A. Amato, and P. J. C. King, Phys. Rev. Lett. **96**, 127202 (2006).

[63] C. Lacroix, P. Mendels, and F. Mila, *Introduction to Frustrated Magnetism: Materials, Experiments, Theory* (Springer Science & Business Media, New York, 2011), Vol. 164.

[64] Y. Li, D. Adroja, P. K. Biswas, P. J. Baker, Q. Zhang, J. Liu, A. A. Tsirlin, P. Gegenwart, and Q. Zhang, Phys. Rev. Lett. **117**, 097201 (2016).

[65] L. Clark, J. C. Orain, F. Bert, M. A. De Vries, F. H. Aidoudi, R. E. Morris, P. Lightfoot, J. S. Lord, M. T. F. Telling, P. Bonville, J. P. Attfield, P. Mendels, and A. Harrison, Phys. Rev. Lett. **110**, 207208 (2013).

[66] S. R. Kreitzman, J. H. Brewer, D. R. Harshman, R. Keitel, D. L. Williams, K. M. Crowe, and E. J. Ansaldo, Phys. Rev. Lett. **56**, 181 (1986).

[67] C. Nisoli, *Frustration(s) and the Ice Rule: From Natural Materials to the Deliberate Design of Exotic Behaviors*, Springer Series in Materials Science (Springer Nature, Switzerland, 2018), pp. 57–59.

[68] R. Yu, O. Nohadani, S. Haas, and T. Roscilde, Phys. Rev. B **82**, 134437 (2010).

[69] T. Roscilde, Phys. Rev. B **74**, 144418 (2006).

[70] H. J. Changlani, S. Ghosh, S. Pujari, and C. L. Henley, Phys. Rev. Lett. **111**, 157201 (2013).

[71] E. Westerberg, A. Furusaki, M. Sigrist, and P. A. Lee, Phys. Rev. Lett. **75**, 4302 (1995).

[72] In Ref. [27], data collapse has been shown for the as-measured specific heat data (without any subtraction of lattice or nuclear/electron Schottky contribution) of Herbertsmithite with $\gamma = 0.5$. Plotting our data (see Fig. 4 in the Supplemental Material [Ref. 40]) in this manner is consistent with $\gamma = 0.5$.